[BMIm][BARF] imidazolium salt solutions in alkyl carbonate solvents: structure and interactions

Marianna Mamusa[1], David Chelazzi[1], Sergio Murgia[2], Emiliano Fratini[1], David Rivillo[3], Henri S. Schrekker[3*], Piero Baglioni[1*]

[1] *Department of Chemistry "Ugo Schiff" and CSGI, University of Florence, Via della Lastruccia 3, Sesto Fiorentino, 50019 Florence, Italy*

[2] *Dipartimento di Scienze Chimiche e Geologiche, Università degli Studi di Cagliari, S.S. 554 Bivio per Sestu, 09042 Monserrato (CA), Italy*

[3] *Institute of Chemistry, Universidade Federal do Rio Grande do Sul, Av. Bento Gonçalves 9500, Porto Alegre, RS, 91501-970, Brazil*

Corresponding Authors

* E-mail: baglioni@csgi.unifi.it; henri.schrekker@ufrgs.br

DOI: 10.1016/j.apmt.2023.101741.

Abstract

Ionic liquids (ILs) have gained growing attention in the past decades, and the focus has recently shifted towards weakly coordinating anions, as in 1-*n*-butyl-3-methylimidazolium tetrakis[3,5-bis(trifluoromethyl)phenyl]borate, [BMIm][BARF]. Solutions of these ILs in alkyl carbonates are of interest, as the latter are "green" solvents with high solvation power. Despite this, the phase behavior and structure of IL solutions in organic polar solvents is still poorly understood. To help fill this knowledge gap, we provide here a study of the interactions and nanoscale structure of [BMIm][BARF] in three symmetrical alkyl carbonate solvents with increasing alkyl chain-length, dimethyl-, diethyl-, and dibutyl carbonate. Electrical conductivity and nuclear magnetic resonance measurements showed that [BMIm][BARF] was mostly undissociated in these solvents, but increased aggregation at the nano-scale occurred in carbonates with higher dielectric constants, as corroborated by small angle X-ray scattering patterns and the analysis of the solvents' carbonyl stretching band via Fourier transform infrared spectroscopy. Such trend is opposite to those previously found for BMIm ILs with less bulky counterions. Because the bulky $BARF^-$ is weakly coordinating and has no ability to give strong H-bonding, short-range anisotropic van der Waals forces are likely key in the interaction of ionic pairs. In this case, some mobility would be required for close contact between ions, and the slower ions self-diffusion in alkyl carbonates with lower dielectric constants might partially hinder self-assembly into local nano-sized structures. Overall, our results shed some light on the interaction and self-organization mechanisms in imidazolium salt-alkyl carbonate mixtures with promising impact in many applicative fields spanning from batteries, catalysis and extraction, up to bio-applications (antimicrobial and bioengineering).

Keywords: imidazolium salts, alkyl carbonates, ionic liquids, [BMIm][BARF], nanostructure

Introduction

Ionic liquids (ILs), a class of compounds composed exclusively of ions, have gained growing attention in the past decades thanks to several interesting properties, such as negligible vapor pressure, nonflammability, and the ideally infinite anion/cation combinations that earned them the definition of "designer solvents".[1,2] This promoted their widespread use in a large number of applications: among others, in analytical and extraction techniques,[3] catalysis,[4] as nanoreactors for colloidal templates,[5] in the preparation of functional gels,[6] in superparamagnetic fluids,[7] and conducting polymer composites.[8] Among the most extensively investigated types of ILs are those based on the *N,N*-dialkyl-substituted imidazolium cation, for which an extensive body of fundamental studies exists;[9] common anions are small inorganic species such as simple halides, tetrafluoroborate, hexafluorophosphate, and bis(trifluoromethylsulfonyl)imide.[10] Recently, the focus has shifted towards anions that show lower tendency to coordinate the cation owing to their bulky structures.[11] This is of significance, for instance, in electrochemical applications where the use of weakly coordinating anions can increase battery current and provide higher stability.[12] The use of ILs as electrolytes for improved batteries has been evaluated for some time now,[13,14] especially in systems based on polar organic solvents providing high conductivity, reduced viscosity, and a wide electrochemical window.[15–19] Among these, alkyl carbonates have been extensively used as solvents and co-solvents in electrochemical applications, thanks to their ability to solvate ions [15] and their environmentally friendly profile as "green" solvents.[20]

Nevertheless, the importance of understanding the phase behavior and nanoscale structure of IL solutions in organic polar solvents has only recently been addressed.[15,19,21–24] The molecular and supramolecular properties of these systems originate from a rich and complex ensemble of forces, including ionic, dipolar, hydrogen bonding, dispersive, and π-π interactions.[15] The study of mixtures of ILs and organic solvents is therefore not always straightforward and still poorly explored.[25]

To help fill this knowledge gap, in this work we investigated the solution properties of the IL 1-*n*-butyl-3-methyl-imidazolium tetrakis[3,5-bis(trifluoromethyl)phenyl]borate, [BMIm][BARF] (whose molecular structure is reported in Figure 1),[26,27] in three alkyl carbonate "green" solvents: dimethyl-, diethyl-, and dibutyl carbonate (DMC, DEC, and DBC). The $BARF^-$ anion presents a rather bulky structure with a tetrahedral geometry around the central boron atom; in addition, electronic charge is dispersed strongly, which hinders coordination bonds. Contrary to the IL containing the similar tetraphenylborate anion, in which the bulky trifluoromethyl substituents are absent, there is no evidence of hydrogen bonding between the BARF anion and the BMIm cation,[26] suggesting that BARF can be classified as non-coordinating anion owing to a combination of steric and strong electronic effect. In particular, we estimated the fraction of dissociated IL by comparing the molar conductivity values obtained by electric conductivity and nuclear magnetic resonance diffusion measurements, while the nanostructural and supramolecular features of the solutions were evaluated by means of small- and wide-angle X-ray scattering, as well as Fourier transform infrared spectroscopy, in an effort to rationalize the relationship between transport properties and the nanoscale structure of [BMIm][BARF] solutions in alkylcarbonate solvents.

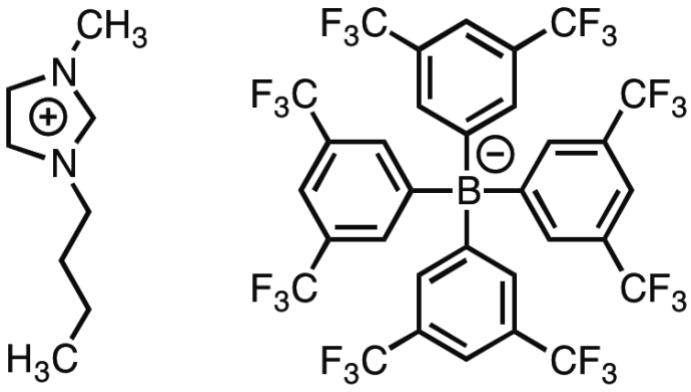

Figure 1. Chemical structure of the IL 1-*n*-butyl-3-methyl-imidazolium tetrakis[3,5-bis(trifluoromethyl)phenyl]borate [BMIm][BARF].

Materials and Methods

The IL 1-*n*-butyl-3-methyl-imidazolium tetrakis[3,5-bis(trifluoromethyl)phenyl]borate, abbreviated [BMIm][BARF], was prepared in 56% isolated yield according to the procedure described by Finden *et al.*[26] ^{1}H NMR ($CDCl_3$) δ 7.78 (m, 1H), 7.68 (m, 8H), 7.53 (m, 4H), 7.02 (m, 1H), 6.93 (m, 1H), 3.94 (t, 2H, ^{3}J = 7.6 Hz), 3.65 (s, 3H), 1.74 (m, 2H), 1.24 (m, 2H), 0.91 (t, 3H, ^{3}J = 7.6 Hz). $C_{80}H_{54}B_2F_{48}N_4$, *MW* = 2004.89 g.mol^{-1}, M_p = 104 °C.

Dimethyl carbonate (DMC, ≥ 99%; *MW* = 90.08 g.mol^{-1}), diethyl carbonate (DEC, ≥ 99%; *MW* = 118.13 g.mol^{-1}) and dibutyl carbonate (DBC, ≥ 99%; *MW* = 174.24 g.mol^{-1}) were purchased from Sigma-Aldrich and used without further purification.

Sample's preparation

Solutions of [BMIm][BARF] in DMC, DEC and DBC were prepared at concentrations of 5, 10, 30, 50 and 70% (wt%) for each solvent, preparing 0.5 g for each solution in glass vials. The vials were sealed with parafilm and stored at 25 °C (± 0.5 °C) for the entire duration of the study. Two weeks were allowed for equilibration before measurements.

Electrical conductivity

The electrical conductivity (σ) of the [BMIm][BARF] solutions in alkyl carbonate solvents was measured at 25 °C using a S230 SevenCompact conductivity meter (Mettler-Toledo) with ± 0.5% accuracy, and a micro conductivity cell (InLab 751-4mm, Mettler-Toledo) equipped with two platinum poles, a chemical resistant glass body, and integrated temperature probe. The cell constant was calibrated with a standard 0.01 M KCl solution.

Nuclear magnetic resonance (NMR)

A Bruker Avance 300 MHz (7.05 T) spectrometer with a ^{1}H operating frequency of 300.131 MHz was used to measure the IL alkyl carbonate solutions. The field gradients (up to 1.2 T m) necessary to measure the self-diffusion coefficients were generated by a Bruker DIFF30 probe supplied by a Bruker Great 1/40 amplifier. All the measurements were carried out at 25 °C, and the temperature was kept constant (with an accuracy of 0.5 °C) by means of a Bruker Variable Temperature unit (BVT 3000). The pulsed gradient stimulated echo (PGSTE) sequence was used. Self-diffusion coefficients were obtained by varying the gradient strength (g) while keeping the gradient pulse length (δ) and the gradient pulse intervals constant within each experimental run. The Stejskal−Tanner equation (Eq. 1) was used to fit recorded data:[28]

$$\frac{I}{I_0} = exp^{[-Dq^2(\Delta-\delta/3)]} \quad (1)$$

where, I and I_0 are the NMR signal intensities in the presence or absence of the applied field gradient, $q = \gamma g \delta$ is the scattering vector (γ is the gyromagnetic ratio of the observed nucleus), ($\Delta - \delta/3$) is the diffusion time, Δ is the delay time between the encoding/decoding gradients, and D is the self-diffusion coefficient to be calculated.

Small- and wide-angle X-ray scattering (SWAXS)

SWAXS experiments were performed on an S3micro X-ray system from Hecus GMBH (Graz), equipped with an ultra-brilliant point microfocus source Genix-Fox 3D (Xenocs, Grenoble). The impinging radiation was the 1.542 Å CuKα, produced by a sealed-tube generator (Seifert ID-303) operating at 2 kW. The detectors (OED 50 M) contained 1024 channels of 54 μm width, and the sample-to-detector distance was 280 mm. The primary beam was masked by a 2 mm W filter allowing

for a Q-range 0.009-0.54 $Å^{-1}$. Samples were placed either in a quartz Mark capillary (2 mm diameter) or a paste sample holder. Measurements were performed under vacuum at 25.0 ± 0.1 °C (temperature controlled by a Peltier element). The resulting scattered intensity I(Q) was plotted as a function of the scattering vector Q, whose modulus is equal to $4\pi \sin \theta/\lambda$, with θ being the angle between the incident and scattered beams. Data reduction and modelling were carried out with Igor Pro (Wavemetrics, Inc.), using the analysis suite developed at the NIST Center for Neutron Research.[29] The scattering length densities of [BMIm][BARF] and the alkyl carbonate solvents (DMC, DEC, DBC) are listed in Table 1.

Table 1. Scattering length density (SLD, ρ) values for the compounds used in this work.

Compound	**SLD, ρ ($Å^{-2}$)**
[BMIm][BARF]	1.30×10^{-05}
DMC	9.61×10^{-06}
DEC	8.91×10^{-06}
DBC	8.59×10^{-06}

Attenuated total reflectance Fourier transform infrared spectroscopy (ATR-FTIR)

ATR-FTIR analysis was carried out on alkyl carbonates and their IL solutions using a ThermoNicolet Nexus 870 equipped with a Golden Gate diamond cell and a MCT detector (Mercury Cadmium Tellurium). The spectra were recorded between 650 and 4000 cm^{-1}, with a spectral resolution of 4 cm^{-1} and 128 scans for each spectrum. Each IL solution was analyzed in quadruplet, and the average spectrum calculated. The spectra of each series of IL solutions (in DBC, DEC and DMC) were normalized to the most intense CH stretching absorption of the corresponding alkyl carbonate (DBC: 2960 cm^{-1}; DEC: 2985 cm^{-1}; DMC: 2962 cm^{-1}).

Results and Discussion

[BMIm][BARF] formed homogeneous mixtures with each of the three alkylcarbonate solvents at all tested concentrations up to 70%, appearing as macroscopically isotropic solutions with increasing viscosity. Instead, over 70%, a phase separation was observed at higher concentrations. It is worth mentioning that, in preliminary tests, similar mixtures of [BMIm][BARF] were also prepared in propylene carbonate (PC), the most common carbonate solvent used as battery electrolyte medium, and the same type of macroscopic phase behavior was observed as with DMC, DEC and DBC; however, the study of the PC solutions was not pursued further since they cannot be investigated by X-ray scattering, due to [BMIm][BARF] and PC having almost identical scattering length density (SLD) values.

Most studies investigating mixtures of ILs with organic polar solvents aim to evaluate their properties as possible battery electrolytes, with the organic solvents acting as media to increase conductivity by two distinct actions: i) reduction of the IL's viscosity, and ii) separation of the IL ion pair by solvation of the individual ions. With such purpose in mind, conductivity measurements of the [BMIm][BARF] stable solutions (5-70 wt%) in DMC, DEC, and DBC were performed. The values of electric conductivity (σ) followed the usual trend found in the literature, *i.e.*, the conductivity increased initially with IL concentration in each solvent, and then decreased after reaching a maximum from 50% to 70% IL content (see Table 2).[23,30] The σ values were in general in the order of 1-5 mS, evidencing poor transport properties in these systems. For a better understanding of this behavior, the calculated molar conductivities (Λ) were compared to those extrapolated from the NMR self-diffusion coefficients of the anion and the cation (Λ_{NMR}) using the Nerst-Einstein equation (Eq. 2):[31]

$$\Lambda_{NMR} = \frac{F^2}{RT}(D_+ + D_-) \qquad (2)$$

where F is the Faraday constant, R is the gas constant, T is the temperature, and $D_{\pm}$ are the self-diffusion coefficients of the ions obtained by PGSTE NMR experiments (also given in Table 2).

Table 2. Molarity (M), electric conductivity (σ) and corresponding molar conductivity (Λ), diffusion coefficients for the cation (D_+) and the anion (D_-), and corresponding extrapolated molar conductivity (Λ_{NMR}), for all the solutions investigated in this paper. DMC = dimethyl carbonate; DEC = diethyl carbonate; DBC = dibutyl carbonate. Standard errors on the final Λ/Λ_{NMR} are in the order of 5%.

Solvent	[BMIm][BARF] wt%	M (mol/cm^3)	σ (S/cm)	Λ (S.cm^2/mol)	D_+ (cm^2/s)	D_- (cm^2/s)	Λ_{NMR} (S.cm^2/mol)	Λ/Λ_{NMR}
DMC	5	2.71×10^{-2}	6.40×10^{-4}	2.36×10^{-2}	4.70×10^{-10}	4.21×10^{-10}	3.35×10^{-1}	0.07
	10	5.50×10^{-2}	1.97×10^{-3}	3.58×10^{-2}	4.70×10^{-10}	4.14×10^{-10}	3.32×10^{-1}	0.11
	30	1.76×10^{-1}	5.50×10^{-3}	3.12×10^{-2}	3.85×10^{-10}	2.96×10^{-10}	2.56×10^{-1}	0.12
	50	3.15×10^{-1}	4.36×10^{-3}	1.39×10^{-2}	2.08×10^{-10}	1.43×10^{-10}	1.32×10^{-1}	0.11
	70	4.75×10^{-1}	1.66×10^{-3}	3.50×10^{-3}	6.75×10^{-10}	3.96×10^{-11}	4.02×10^{-2}	0.09
DEC	5	2.48×10^{-2}	3.15×10^{-4}	1.27×10^{-2}	3.78×10^{-10}	3.98×10^{-10}	2.92×10^{-1}	0.04
	10	5.05×10^{-2}	1.03×10^{-3}	2.04×10^{-2}	3.52×10^{-10}	3.03×10^{-10}	2.46×10^{-1}	0.08
	30	1.64×10^{-1}	3.53×10^{-3}	2.15×10^{-2}	2.64×10^{-10}	2.03×10^{-10}	1.75×10^{-1}	0.12
	50	2.98×10^{-1}	3.61×10^{-3}	1.21×10^{-2}	1.36×10^{-10}	9.72×10^{-11}	8.76×10^{-2}	0.14
	70	4.58×10^{-1}	1.63×10^{-3}	3.56×10^{-3}	3.76×10^{-11}	2.17×10^{-11}	2.23×10^{-2}	0.16
DBC	5	2.39×10^{-2}	6.70×10^{-4}	2.80×10^{-3}	1.37×10^{-10}	1.24×10^{-10}	9.81×10^{-2}	0.03
	10	4.87×10^{-2}	0.26×10^{-3}	5.29×10^{-3}	1.32×10^{-10}	1.19×10^{-10}	9.43×10^{-2}	0.06
	30	1.59×10^{-1}	1.15×10^{-3}	7.23×10^{-3}	9.71×10^{-11}	8.23×10^{-11}	6.74×10^{-2}	0.11
	50	2.91×10^{-1}	1.66×10^{-3}	5.69×10^{-3}	4.22×10^{-11}	3.15×10^{-11}	2.77×10^{-2}	0.21
	70	4.51×10^{-1}	0.57×10^{-3}	1.27×10^{-3}	1.35×10^{-11}	8.21×10^{-12}	8.16×10^{-3}	0.16

Indeed, while the Λ values are the consequence of charged species migrating under the effect of an electric field, Λ_{NMR} values are obtained from Eq. 2 under the assumption that all the diffusing species observed in the NMR experiment, characterized by a unitary activity coefficient, contribute to the calculated molar conductivity. Since ions can exist in solution either as neutral aggregates or as ion pairs, this implicitly means that the Λ/Λ_{NMR} ratio gives the percentage of non-aggregated diffusing

species (solvated ions) contributing to the measured conductivity. Such a piece of information may be helpful in clarifying the transport properties of the studied systems. The very low Λ/Λ_{NMR} ratios reported in Table 2 prove that only a small fraction of [BMIm][BARF] was in ionic form in all the investigated solutions. When DMC was used as solvent, dilution did not significantly affect the degree of ionization. Instead, when [BMIm][BARF] was dissolved in DEC or DBC the degree of ionization was further suppressed upon dilution, a phenomenon that seems to be correlated with the length of the alkyl chain of the solvent, or with its dielectric constant (DMC, DEC, and DBC possess the following dielectric constants: 3.2, 2.8, and 2.6)[32–34].

For a better characterization of the mixtures' structures at the nanoscale, the dynamic information obtained by conductivity measurements was completed by the insights provided by a static technique such as SWAXS. Small angle X-ray scattering (SAXS) results are plotted in Figure 2, where the scattering intensity, I(Q), is a function of the scattering vector Q. The patterns show a common trend: a decreasing forward scattering intensity, *I(0)*, and a change in the shape of scattering with increasing IL content in each solvent. Recent SAXS investigations of IL/organic solvent mixtures have evidenced that the interpretation of such scattering patterns can be complicated by the coexisting nanostructures formed by pure phases of both compounds, generated by the different intermolecular forces at play (Coulombic, dipolar-dipolar, hydrogen bonding, van der Waals),[25] and that systems appearing completely miscible can reveal density and concentration fluctuations at the nanoscale.[35] With this in mind, the curves at 10% IL were modelled using the Ornstein-Zernike equation (Eq. 3),[36] which represents the scattering arising from composition fluctuations:

$$I(Q) = \frac{I(0)}{1+(Q\xi)^2} \quad (3)$$

where ξ is the correlation length of electron density fluctuations. The curve fits are displayed in Figure 2D, while the correlation lengths thereby obtained are reported in Table 3 along with the scattering contrast values for each system and the dielectric constants of the solvents.

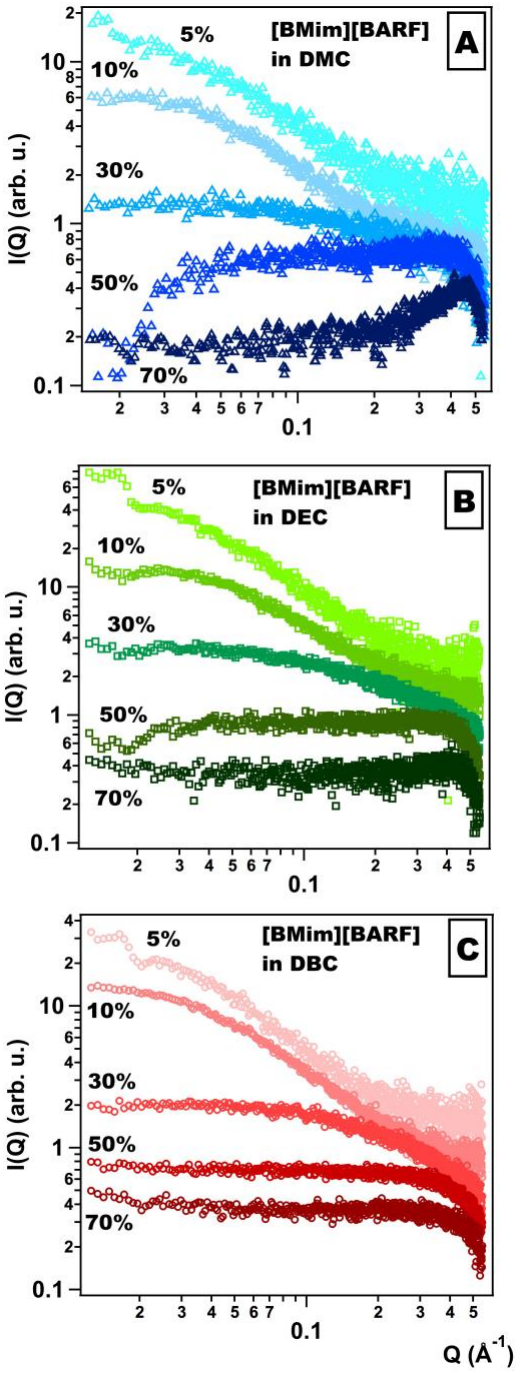

Figure 2. SAXS patterns for [BMIm][BARF] in A) dimethyl carbonate (DMC), B) diethyl carbonate (DEC), and C) dibutyl carbonate (DBC). IL contents (wt%) are indicated next to each curve. The curves have been offset along the y axis to help readability.

Table 3. Correlation lengths ξ (Å) obtained by modelling the SAXS curves of the 10% [BMIm][BARF] solutions (see Figure 2) with Eq. 3; IL/solvent contrasts $\Delta\rho^2$ ($Å^{-4}$) calculated from the SLD values in Table 1; low-frequency dielectric constants at 298 K ([a] from ref. [32]; [b] from ref. [33]; [c] from ref. [34]). DBC = dibutyl carbonate; DEC = diethyl carbonate; DMC = dimethyl carbonate.

Solvent	**Correlation length $\xi \pm 0.6$ (Å)**	**Contrast $\Delta\rho^2$ ($Å^{-4}$)**	**Dielectric constant ε (at 298 K)**
DMC	15.3	1.17×10^{-11}	3.2 [a]
DEC	16.3	1.70×10^{-11}	2.8 [b]
DBC	20.4	1.97×10^{-11}	2.6 [c]

For [BMIm][BARF] contents higher than 10%, a correlation peak appeared at Q ≈ 0.42-0.45 $Å^{-1}$, which is quite evident in the DMC curves, less pronounced in DEC, and barely recognizable in the DBC samples, suggesting a trend that follows the increasing alkyl chain length and the decreasing dielectric constant of the solvent. Such Q position translates into a real-space interaction distance of 13-15 Å. A correlation peak accompanied by decreasing forward scattering intensity is representative of repulsive interactions between objects in solution; since the maximum diameter of the [BMIm][BARF] ion pair is about 20 Å (using the calculated values of 10.9 Å for the anion and 8.6 Å for the stretched cation, estimated with Avogadro software), it is reasonable to assume that the correlation peak might arise from the interactions between undissociated IL pairs in solution. Considering the maximum IL content, 70%, such interaction was definitely more evident in DMC than in DBC, suggesting that for

the same number of IL molecules in solution, a larger number was undissociated in DMC than in DBC. This is in agreement with the trend already observed by analyzing the Λ/Λ_{NMR} values above. It is worth mentioning that we attempted to model these SAXS curves using the available structure factors for some common interaction potentials, *e.g.* screened Coulomb and hard spheres.[37] However, some of the obtained values, particularly the hard sphere volume fraction, were unphysical: this is not entirely unexpected, since the available models have been developed for the interpretation of scattering patterns produced by centro-symmetric, monodisperse objects in aqueous medium, and their application to the present systems carries the risk of overinterpretation of the experimental data.

The FTIR spectra of [BMIm][BARF] in the three solvents were investigated to gain further evidence of the interactions between the different alkyl carbonates and the IL. The FTIR C=O stretching of the alkyl carbonates has a strong and well isolated absorption band in the 1720-1760 cm^{-1} region, which has been used as a probe to investigate the solvation structure and interactions of these solvents with electrolytes.[38] First, we looked into changes in the band's maximum frequency (see Table 4 and Figure 4A); some red shift of the peak was observed (*i.e.*, to lower wavenumbers) for increasing IL concentration above 50%, and the shift was more intense for DBC (ca. 8-9 cm^{-1} at the highest IL concentration) than for DEC (5-6 cm^{-1}, closer to the spectral resolution), while no significant shift could be detected for DMC. A red shift indicates bond elongation, while a blue shift would indicate bond contraction. Thus, the presence of some red shift for increasing IL concentration already suggests that the electrolyte might interfere with the interactions between alkyl carbonate molecules. The red shift observed in DEC and DBC solutions at 70% is in good agreement with the larger values of Λ/Λ_{NMR} found for the same solutions as compared to the other samples, indicating increased solvation of the IL.

Alkyl carbonates are known to associate mainly through C-H···O intermolecular interactions between the carbonyl oxygen of one molecule as proton acceptor and the C-H group of another

molecule as proton donor, and such interactions were classified as hydrogen bonds by Wang *et al.* on the basis of atoms-in-molecules calculations.[39] Instead, according to Finden *et al.*, no H-bonding interactions take place between the imidazolium and the BARF ions, as the bulky trifluoromethyl moieties prevent the anion and cation from coming into close enough proximity for such interactions to occur.[26] It is thus expected that new H-bonding interactions will be established between the alkyl carbonates and the IL, possibly through the carbonate group and the mildly acidic proton in position C2 of the imidazolium cation.[40,41]

Indeed, a significant broadening of the C=O stretching band was observed for the different carbonates, and two trends are evident (see Table 4 and Figure 4B): i) the band full width at half maximum (FWHM) increased with increasing IL concentration, and ii) the band broadening at the highest IL concentrations (50-70 wt%) follows the trend DBC ≥ DEC >> DMC. In order to separate the effect of carbonate dilution from that of solvent-IL interaction, the spectra of each IL solution were normalized to the most intense CH stretching absorption of the alkyl carbonates, which is justified considering that solvation strongly affects the stretching and bending modes of C=O and C-O-C groups of the carbonate solvents.[42] However, it must be noticed that the same trends were observed in the spectra even before normalization, which suggests that the effect of solvent-IL interaction is prevalent.

Width increases of the carbonyl band were previously reported by Deepa *et al.* for PC interacting with lithium imide,[43] and by Fulfer *et al.* for the interaction of linear organic carbonates with lithium hexafluorophosphate.[38] In the first case, it was found that the bandwidths of the well-separated components of the Fermi doublet of the PC C=O stretching band increased with increasing salt concentration in the solvent. In the second case, the authors reported that the frequency distribution of the carbonyl stretch was broadened as the alkyl chain length was increased, likely due to the increased number of possible conformers for carbonate molecules with longer alkyl chains. Therefore, it seems

reasonable to hypothesize that also in the case of interactions of alkyl carbonates with [BMIm][BARF], DBC has the most disordered solvation shell, followed by DEC and DMC.

Overall, our combined NMR, SAXS and FTIR data consistently point to increased aggregation of [BMIm][BARF] in alkyl carbonates with higher dielectric constants (DMC > DEC > DBC). This behavior is opposite to that reported previously for [BMIm][BF_4] and [BMIm][PF_6]: in several studies [30,44] involving a wide range of solvents (water, ethanol, DMSO, acetonitrile and THF), increased aggregation was found for lower dielectric constants. A possible explanation might rely on how the aggregation drives changes in different BMIm ILs. Because the local structure of nano-sized IL aggregates does not explicitly depend on long-range electrostatic interactions [45], IL units require some mobility to come close and initiate self-assembly. Instead, larger structures of the liquids (*i.e.*, collection of nano-sized aggregates) will be influenced by long-range dipole-dipole interactions [45]. For pairs with less bulky counterions (higher mobility) and strong H-bonding, aggregation is thus mostly driven by electrostatic forces, and stronger aggregation comes from reduced screening in solvents with lower dielectric constants. This would be in line with the work of Osti *et al.*,[15] who explained the increased ion dissociation of [BMIm][Tf_2N] with increasing solvent polarity by a more efficient screening of the electrostatic interactions, in particular in IL-rich phases. Instead, in the case of bulky and weakly interacting counterions such as BARF, short-range anisotropic van der Waals forces are likely key in the interaction of ionic pairs, and the intrinsic low mobility of the BARF anions might partially hinder their assembly with BMIm; mobility seems to be further reduced in solutions of the IL in alkyl carbonates with increasingly lower dielectric constants (see the trends of anion self-diffusion coefficients, D_-, in Table 2), and possibly less assembly (aggregation) takes place.

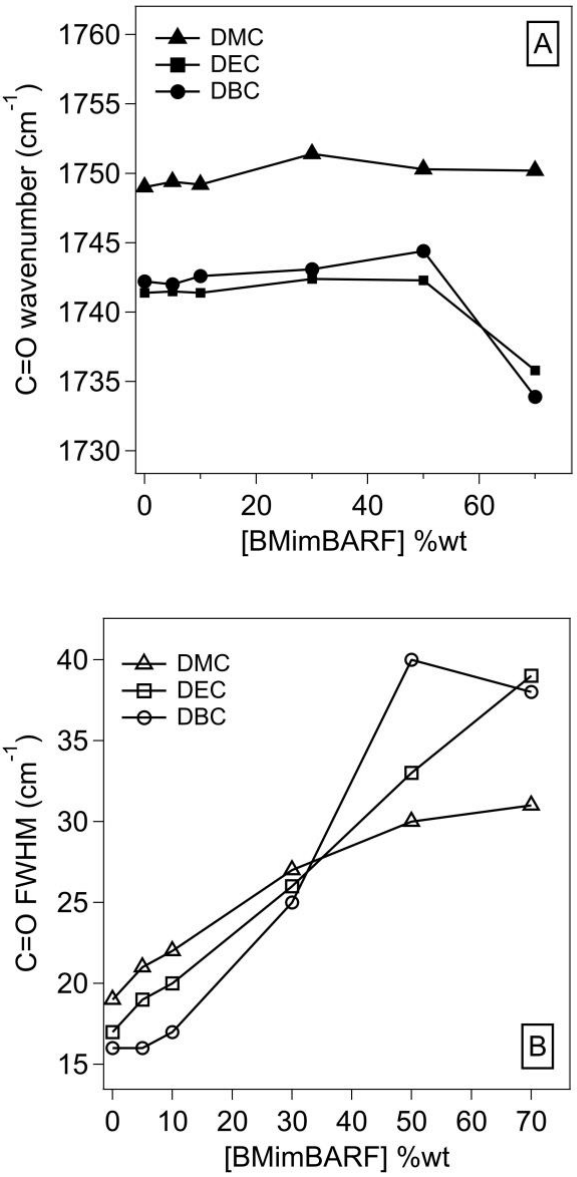

Figure 4. A) Position (wavenumber) and B) full width at half maximum (FWHM) of the FTIR C=O stretching band of alkyl carbonates (1720-1760 cm^{-1}), in the presence of [BMIm][BARF] at different concentrations. DBC = dibutyl carbonate; DEC = diethyl carbonate; DMC = dimethyl carbonate.

Table 4. Position (wavenumber) and full width at half maximum (FWHM) of the C=O stretching band of alkyl carbonates in solution with [BMIm][BARF], at different concentrations. DBC = dibutyl carbonate; DEC = diethyl carbonate; DMC = dimethyl carbonate. The error on wavenumbers is ca. ± 0.3 cm^{-1} (lower than the spectral resolution of 4 cm^{-1}), while that on FWHM is ca. ± 1 cm^{-1}.

IL concentration (wt%)	DBC wavenumber (cm^{-1})	DBC FWHM (cm^{-1})	DEC wavenumber (cm^{-1})	DEC FWHM (cm^{-1})	DMC wavenumber (cm^{-1})	DMC FWHM (cm^{-1})
0	1742.4	16	1741.4	17	1749.0	19
5	1742.0	16	1741.5	19	1749.4	21
10	1742.6	17	1741.4	20	1749.2	22
30	1743.1	25	1742.4	26	1751.4	27
50	1744.4	40	1742.3	33	1750.3	30
70	1733.9	38	1735.8	39	1750.2	31

Conclusions

This work aimed to provide fundamental insight in the multiscale structure and interactions of solutions of the IL [BMIm][BARF] in three alkylcarbonate solvents, i.e., dimethyl-, diethyl-, and dibutylcarbonate. The estimation of the molar conductivity ratio Λ/Λ_{NMR} showed that the IL was mostly undissociated in these solvents. However, some trends emerged as the solvent was changed along the series DMC-DEC-DBC. Our data seem to suggest increased aggregation of the IL in solvents with higher dielectric constants; not only this is evident from the Λ/Λ_{NMR} values, but also trends of SAXS patterns and FTIR analysis of the carbonyl stretching bands provide a corroborating picture. Our findings are opposite to those found by previous studies on BMIm ILs with less bulky counterions, where increased aggregation was found to occur in solvents with lower dielectric constants. We

hypothesize that the nature of the BMIm counterion might play a fundamental role in the assembly of the ions to form nano-sized aggregates. BARF is a weakly coordinating anion with no ability to give strong H-bonding, thus short-range anisotropic van der Waals forces are likely key in the interaction of ionic pairs; in this case, some mobility would be required for close contact between ions, and the slower ions self-diffusion in alkyl carbonates with lower dielectric constants might partially hinder self-assembly into local nano-sized droplets. In this picture, it is evident that a complex intermix of molecular forces is at play to finely tune the interactions between different species and the resulting nanostructures. When a series of solvents of similar dielectric properties is considered, the otherwise subtle role of dispersion forces and, in the present case, hydrogen bonding vs. van der Waals interactions, can become important enough to reverse the order of solvation capability expected by considering merely the electrostatic component to the interaction potential. This knowledge impacts positively on the understanding of ionic liquid solutions in organic solvents, providing new perspectives in, *e.g.*, electrochemistry, nanoscience and nanotechnology.

Acknowledgements

The European Union Horizon 2020 project APACHE (Active & Intelligent Packaging Materials and Display Cases as a Tool for Preventive Conservation of Cultural Heritage), under the Horizon 2020 Research and Innovation Programme Grant Agreements 814496, is gratefully acknowledged for the financial support. MUR (PRIN 2017249YEF) and CSGI are also acknowledged for funding this work. The Conselho Nacional de Desenvolvimento Científico e Tecnológico - Brasil (CNPq) is acknowledged for financial support. Henri S. Schrekker is grateful to CNPq for the research productivity PQ fellowship.

References

[1] H. Niedermeyer, J.P. Hallett, I.J. Villar-Garcia, P.A. Hunt, T. Welton, Mixtures of ionic liquids, Chem. Soc. Rev. 41 (2012) 7780-7802. https://doi.org/10.1039/c2cs35177c.
[2] S.K. Singh, A.W. Savoy, Ionic liquids synthesis and applications: An overview, J. Mol. Liq. 297 (2020) 112038. https://doi.org/10.1016/j.molliq.2019.112038.
[3] K. Yavir, Ł. Marcinkowski, R. Marcinkowska, J. Namieśnik, A. Kloskowski, Analytical applications and physicochemical properties of ionic liquid-based hybrid materials: A review, Anal Chim. Acta. 1054 (2019) 1–16. https://doi.org/10.1016/j.aca.2018.10.061.

[4] R.L. Vekariya, A review of ionic liquids: Applications towards catalytic organic transformations, J. Mol. Liq. 227 (2017) 44–60. https://doi.org/10.1016/j.molliq.2016.11.123.
[5] M. Mamusa, M.C. Arroyo, E. Fratini, R. Giorgi, P. Baglioni, Nonaqueous Microemulsion in the $BmimTf_2N$/Brij 30/n-Nonane System: Structural Investigation and Application as Gold Nanoparticle Microreactor, Langmuir. 34 (2018) 12609–12618. https://doi.org/10.1021/acs.langmuir.8b02420.
[6] P.C. Marr, A.C. Marr, Ionic liquid gel materials: applications in green and sustainable chemistry, Green Chem. 18 (2016) 105–128. https://doi.org/10.1039/C5GC02277K.
[7] M. Mamusa, J. Sirieix-Plénet, R. Perzynski, F. Cousin, E. Dubois, V. Peyre, Concentrated assemblies of magnetic nanoparticles in ionic liquids, Faraday Discuss. 181 (2015) 193–209. https://doi.org/10.1039/C5FD00019J.
[8] B.G. Soares, Ionic liquid: A smart approach for developing conducting polymer composites, J. Mol. Liq. 262 (2018) 8–18. https://doi.org/10.1016/j.molliq.2018.04.049.
[9] J. Dupont, On the solid, liquid and solution structural organization of imidazolium ionic liquids, J. Braz. Chem. Soc. 15 (2004) 341–350. https://doi.org/10.1590/S0103-50532004000300002.
[10] H. Xue, R. Verma, J.M. Shreeve, Review of ionic liquids with fluorine-containing anions, J. Fluor. Chem. 127 (2006) 159–176. https://doi.org/10.1016/j.jfluchem.2005.11.007.
[11] M. Kaliner, T. Strassner, Tunable aryl alkyl ionic liquids with weakly coordinating bulky borate anion, Tetrahedron Lett. 57 (2016) 3453–3456. https://doi.org/10.1016/j.tetlet.2016.06.082.
[12] I. Krossing, I. Raabe, Noncoordinating Anions—Fact or Fiction? A Survey of Likely Candidates, Angew. Chem. Int. Ed. 43 (2004) 2066–2090. https://doi.org/10.1002/anie.200300620.
[13] D.R. MacFarlane, N. Tachikawa, M. Forsyth, J.M. Pringle, P.C. Howlett, G.D. Elliott, J.H. Davis, M. Watanabe, P. Simon, C.A. Angell, Energy applications of ionic liquids, Energy Environ. Sci. 7 (2014) 232–250. https://doi.org/10.1039/C3EE42099J.
[14] A.B. McEwen, Nonaqueous Electrolytes for Electrochemical Capacitors: Imidazolium Cations and Inorganic Fluorides with Organic Carbonates, J. Electrochem. Soc. 144 (1997) L84-L86. https://doi.org/10.1149/1.1837561.
[15] N.C. Osti, K.L. Van Aken, M.W. Thompson, F. Tiet, D. Jiang, P.T. Cummings, Y. Gogotsi, E. Mamontov, Solvent Polarity Governs Ion Interactions and Transport in a Solvated Room-Temperature Ionic Liquid, J. Phys. Chem. Lett. 8 (2017) 167–171. https://doi.org/10.1021/acs.jpclett.6b02587.
[16] R.A. Di Leo, A.C. Marschilok, K.J. Takeuchi, E.S. Takeuchi, Battery electrolytes based on saturated ring ionic liquids: Physical and electrochemical properties, Electrochim. Acta. 109 (2013) 27–32. https://doi.org/10.1016/j.electacta.2013.07.041.
[17] K. Gao, X.-H. Song, Y. Shi, S.-D. Li, Electrochemical performances and interfacial properties of graphite electrodes with ionic liquid and alkyl-carbonate hybrid electrolytes, Electrochim. Acta. 114 (2013) 736–744. https://doi.org/10.1016/j.electacta.2013.10.118.
[18] L. Lombardo, S. Brutti, M.A. Navarra, S. Panero, P. Reale, Mixtures of ionic liquid – Alkylcarbonates as electrolytes for safe lithium-ion batteries, J. Power Sources. 227 (2013) 8–14. https://doi.org/10.1016/j.jpowsour.2012.11.017.
[19] P.H. Lam, A.T. Tran, D.J. Walczyk, A.M. Miller, L. Yu, Conductivity, viscosity, and thermodynamic properties of propylene carbonate solutions in ionic liquids, J. Mol. Liq. 246 (2017) 215–220. https://doi.org/10.1016/j.molliq.2017.09.070.
[20] P. Tundo, New developments in dimethyl carbonate chemistry, Pure Appl. Chem. 73 (2001) 1117–1124. https://doi.org/10.1351/pac200173071117.

[21] M. Kim, I.-J. Kim, S. Yang, S. Kim, Electrochemical properties of organic electrolyte solutions containing 1-ethyl-3-methylimidazolium tetrafluoroborate salt, Res. Chem. Intermed. 41 (2015) 4749–4759. https://doi.org/10.1007/s11164-014-1565-1.
[22] M. Vraneš, N. Zec, A. Tot, S. Papović, S. Dožić, S. Gadžurić, Density, electrical conductivity, viscosity and excess properties of 1-butyl-3-methylimidazolium bis(trifluoromethylsulfonyl)imide+propylene carbonate binary mixtures, J. Chem. Thermodyn. 68 (2014) 98–108. https://doi.org/10.1016/j.jct.2013.08.034.
[23] A. Stoppa, J. Hunger, R. Buchner, Conductivities of Binary Mixtures of Ionic Liquids with Polar Solvents †, J. Chem. Eng. Data. 54 (2009) 472–479. https://doi.org/10.1021/je800468h.
[24] A.B. Pereiro, E. Tojo, A. Rodríguez, J. Canosa, J. Tojo, Properties of ionic liquid HMIMPF$_6$ with carbonates, ketones and alkyl acetates, J. Chem. Thermodyn. 38 (2006) 651–661. https://doi.org/10.1016/j.jct.2005.07.020.
[25] T. Murphy, R. Hayes, S. Imberti, G.G. Warr, R. Atkin, Ionic liquid nanostructure enables alcohol self assembly, Phys. Chem. Chem. Phys. 18 (2016) 12797–12809. https://doi.org/10.1039/C6CP01739H.
[26] J. Finden, G. Beck, A. Lantz, R. Walsh, M.J. Zaworotko, R.D. Singer, Preparation and characterization of 1-butyl-3-methylimidazolium tetrakis(3,5-bis(trifluoromethyl)phenyl)borate, [bmim]BARF, J. Chem. Crystallogr. 33 (2003) 287–295. https://doi.org/10.1023/A:1023885212233.
[27] W. Levason, D. Pugh, G. Reid, Imidazolium-based ionic liquids with large weakly coordinating anions, New J. Chem. 41 (2017) 1677–1686. https://doi.org/10.1039/C6NJ03674K.
[28] S. Murgia, G. Palazzo, M. Mamusa, S. Lampis, M. Monduzzi, Aerosol-OT Forms Oil-in-Water Spherical Micelles in the Presence of the Ionic Liquid bmimBF$_4$, J. Phys. Chem. B. 113 (2009) 9216–9225. https://doi.org/10.1021/jp902970n.
[29] S.R. Kline, Reduction and analysis of SANS and USANS data using IGOR Pro, J. Appl. Crstallogr. 39 (2006) 895–900. https://doi.org/10.1107/S0021889806035059.
[30] W. Li, Z. Zhang, J. Zhang, B. Han, B. Wang, M. Hou, Y. Xie, Micropolarity and aggregation behavior in ionic liquid+organic solvent solutions, Fluid Ph. Equilibria. 248 (2006) 211–216. https://doi.org/10.1016/j.fluid.2006.08.013.
[31] H. Tokuda, S. Tsuzuki, Md. A.B.H. Susan, K. Hayamizu, M. Watanabe, How Ionic Are Room-Temperature Ionic Liquids? An Indicator of the Physicochemical Properties, J. Phys. Chem. B. 110 (2006) 19593–19600. https://doi.org/10.1021/jp064159v.
[32] R. Naejus, D. Lemordant, R. Coudert, P. Willmann, Excess thermodynamic properties of binary mixtures containing linear or cyclic carbonates as solvents at the temperatures 298.15 K and 315.15 K, J. Chem. Thermodyn. 29 (1997) 1503–1515. https://doi.org/10.1006/jcht.1997.0260.
[33] L. Mosteiro, E. Mascato, B.E. de Cominges, T.P. Iglesias, J.L. Legido, Density, speed of sound, refractive index and dielectric permittivity of (diethyl carbonate + n - decane) at several temperatures, J. Chem. Thermodyn. 33 (2001) 787–801. https://doi.org/10.1006/jcht.2000.0779.
[34] D. Saar, J. Brauner, H. Farber, S. Petrucci, Ultrasonic and microwave dielectric relaxation of liquid dialkyl carbonates, J. Phys. Chem. 82 (1978) 2531–2535. https://doi.org/10.1021/j100512a014.
[35] O. Russina, A. Sferrazza, R. Caminiti, A. Triolo, Amphiphile Meets Amphiphile: Beyond the Polar–Apolar Dualism in Ionic Liquid/Alcohol Mixtures, J. Phys. Chem. Lett. 5 (2014) 1738–1742. https://doi.org/10.1021/jz500743v.
[36] A. Guinier, G. Fournet, C.B. Walker, Small angle scattering of X-rays, J. Wiley&Sons, New York, 1955.

[37] O. Glatter, O. Kratky, eds., Small angle x-ray scattering, Academic Press, London; New York, 1982.
[38] K.D. Fulfer, D.G. Kuroda, A comparison of the solvation structure and dynamics of the lithium ion in linear organic carbonates with different alkyl chain lengths, Phys. Chem. Chem. Phys. 19 (2017) 25140–25150. https://doi.org/10.1039/C7CP05096H.
[39] Y. Wang, P.B. Balbuena, Associations of Alkyl Carbonates: Intermolecular C−H···O Interactions, J. Phys. Chem. A. 105 (2001) 9972–9982. https://doi.org/10.1021/jp0126614.
[40] A. Wulf, K. Fumino, R. Ludwig, Spectroscopic Evidence for an Enhanced Anion–Cation Interaction from Hydrogen Bonding in Pure Imidazolium Ionic Liquids, Angew. Chem. Int. Ed. 49 (2010) 449–453. https://doi.org/10.1002/anie.200905437.
[41] K. Dong, S. Zhang, D. Wang, X. Yao, Hydrogen Bonds in Imidazolium Ionic Liquids, J. Phys. Chem. A. 110 (2006) 9775–9782. https://doi.org/10.1021/jp054054c.
[42] L. Doucey, M. Revault, A. Lautié, A. Chaussé, R. Messina, A study of the Li/Li+ couple in DMC and PC solvents, Electrochim. Acta. 44 (1999) 2371–2377. https://doi.org/10.1016/S0013-4686(98)00365-X.
[43] M. Deepa, S.A. Agnihotry, D. Gupta, R. Chandra, Ion-pairing effects and ion–solvent–polymer interactions in $LiN(CF_3SO_2)_2$–PC–PMMA electrolytes: a FTIR study, Electrochim. Acta. 49 (2004) 373–383. https://doi.org/10.1016/j.electacta.2003.08.020.
[44] H.K. Stassen, R. Ludwig, A. Wulf, J. Dupont, Imidazolium Salt Ion Pairs in Solution, Chem. Eur. J. 21 (2015) 8324–8335. https://doi.org/10.1002/chem.201500239.
[45] B. Shadrack Jabes, L. Delle Site, Nanoscale domains in ionic liquids: A statistical mechanics definition for molecular dynamics studies, J. Chem. Phys. 149 (2018) 184502, 1-9. https://doi.org/10.1063/1.5054999.